Dose-dependent biological damage of tumour cells by laser-accelerated proton beams

To cite this article: S D Kraft *et al* 2010 *New J. Phys.* **12** 085003

View the article online for updates and enhancements.

Dose-dependent biological damage of tumour cells by laser-accelerated proton beams

S D Kraft[1], **C Richter**[1,2], **K Zeil**[1], **M Baumann**[2,3], **E Beyreuther**[1], **S Bock**[1], **M Bussmann**[1], **T E Cowan**[1], **Y Dammene**[1,2], **W Enghardt**[1,2,3], **U Helbig**[1], **L Karsch**[2], **T Kluge**[1], **L Laschinsky**[2], **E Lessmann**[1], **J Metzkes**[1], **D Naumburger**[2], **R Sauerbrey**[1], **M. Schürer**[2], **M Sobiella**[1], **J Woithe**[2], **U Schramm**[1,4] **and J Pawelke**[1,2,4]

[1] Forschungszentrum Dresden-Rossendorf (FZD), Bautzner Landstraße 400, 01328 Dresden, Germany
[2] OncoRay—Center for Radiation Research in Oncology, TU Dresden, Fetscherstr. 74, 01307 Dresden, Germany
[3] Klinik für Strahlentherapie und Radioonkologie, TU Dresden, Fetscherstr. 74, 01307 Dresden, Germany
E-mail: u.schramm@fzd.de and joerg.pawelke@oncoray.de

Abstract. We report on the first irradiation of *in vitro* tumour cells with laser-accelerated proton pulses showing dose-dependent biological damage. This experiment, paving the way for future radiobiological studies with laser-accelerated protons, demonstrates the simultaneous availability of all the components indispensable for systematic radiobiological studies: a laser–plasma accelerator providing proton spectra with maximum energy exceeding 15 MeV and applicable doses of a few Gy within a few minutes; a beam transport and filtering system; an in-air irradiation site; and a dosimetry system providing both online dose monitoring and absolute dose information applied to the cell sample and the full infrastructure for analysing radiation-induced damage in cells.

[4] Authors to whom any correspondence should be addressed.

Contents

1. Introduction

The idea of the use of ion (i.e. proton and heavier ions) beams in the radiotherapy of malignant tumours can be most easily understood in terms of their energy transfer characteristics in comparison to widely used x-rays or electrons. Heavily charged particles show in material only little spatial scattering, and in contrast to electrons and x-ray radiation, the dominant part of their kinetic energy is deposited close to the end of their trajectory in the well-known Bragg peak. Generally speaking, these features allow for a more precise irradiation of a tumour at a considerably reduced dose deposition in healthy surrounding tissue. Over the last decade, great progress has been made in this method and due to the superior performance for a number of tumour entities, novel centres are coming into operation presently or within the next few years worldwide ([1]–[3]; see e.g. [4]). However, as the required accelerator and beam transport technology, as well as the radiation shielding for high-energy ion beams, is complex and costly, it has been implemented only in a few large-scale facilities to date, and the demand for more compact and flexible high gradient acceleration and beam transport techniques is evident.

In parallel with these developments in cyclotron or synchrotron acceleration of ions for radiotherapy, laser–plasma acceleration of proton beams has made tremendous progress. A decade ago, large high-power glass lasers operating at a few pulses per day demonstrated intense proton pulses with maximum energies in the range of 60 MeV [5] and triggered several proposals concerning the potential therapeutic applications of such acceleration techniques [6]–[12].

The pulse properties of laser–plasma-accelerated proton beams differ significantly from those commonly provided by medical accelerators in pulse duration, peak current and correspondingly pulse dose rate and energy spectrum. Thus, it has been pointed out [13, 14] that among obvious properties such as operational stability, a reliable and precise physical and dosimetric characterization of laser–plasma-accelerated particle beams has to be established. Moreover, the biological effectiveness of laser-accelerated particles has to be determined and compared to that for established particle sources before starting any medical application. This task requires a whole chain of extensive experiments, starting with systematic *in vitro* cell irradiation, and moving through animal experiments to clinical trials with patients.

However, as basic radiobiological studies already require the repeated irradiation of samples on a minute time scale, only laser systems operating at a repetition rate of at least several

pulses per minute can be used for full-scale experimental studies. With the recent development of 100 TW class Ti:sapphire laser systems running at a pulse repetition rate of up to 10 Hz, maximum proton energies of well above 10 MeV, interesting for radiobiological investigations, have been reached [15] and thus the restricting energy limitations of the previous generation of such table-top laser systems have been overcome.

So far, very few radiobiological investigations of *in vitro* cell damage due to laser-accelerated particles have been carried out. The first systematic experiments were performed with electrons already including a precise absolute dosimetry [16]. For ions, only one qualitative proof-of-principle experiment utilizing protons with low energies between 0.8 and 2.4 MeV has been reported [17]. Complementary experiments aiming at the investigation of the biological effectiveness of short-pulse (few ns) proton beams were recently performed at a conventional tandem Van de Graaf accelerator providing pulsed and continuous modes of 20 MeV protons [18].

In this paper, we describe the first study of cell damage induced by laser-accelerated protons including both online dose monitoring and absolute dose evaluation. Section 2 presents a comprehensive guideline for the non-specialist reader that summarizes the most relevant— and, for the specialist, evident—requirements for the performance of radiobiological *in vitro* experiments on a laser-accelerator-driven cell irradiation site. Section 3 serves as a task list, motivating the choice of the parameters of the laser–plasma accelerator, the magnetic filter device and the dedicated combined dosimetry and cell irradiation device. Full operation of the combined system is demonstrated by the irradiation of tumour cells with three different doses, where a clear trend in the number of DNA double-strand breaks becomes visible in accordance with the delivered dose ratios.

2. Requirements for radiobiological *in vitro* experiments

- As living cells have to be irradiated in air, a vacuum exit window for the proton beam is mandatory.

- Due to the comparatively low energy of presently available laser-accelerated protons ($\sim$10 MeV), all components used in transmission in front of the cell monolayer have to be as thin as possible in order to minimize energy loss.

- All types of background radiation causing cell damage, such as x-rays or electrons, have to be suppressed, e.g., by blocking the direct view from the laser target to the cell sample or by magnetic filtering.

- The delivered proton intensity should be high enough to guarantee irradiation times of the order of a few minutes to avoid the influence of any effects not related to the irradiation.

- In order to derive the biological effectiveness of laser-accelerated proton beams, dose–effect curves with radiation doses in the range of about 0.1–10 Gy have to be measured.

- The large shot-to-shot intensity fluctuations observed up to now for laser-accelerated proton beams as compared to conventional sources make the delivery of a prescribed dose by a single pulse impossible. It requires the application of several pulses in combination with online dose monitoring for each individual irradiation.

- The beam diameter has to be optimized with regard to the geometry of the cell sample. This implies a homogeneous dose distribution over an area typically in the range of about 1–25 cm^2.

- Precise evaluation of the absolute dose delivered by polyenergetic proton beams requires a knowledge of the proton energy spectrum.

- In contrast to the monoenergetic proton beams common in medical applications, no absolute dosimetry protocol exists for the laser-accelerated proton pulses at low energies and therefore one has to be established.

- Precise absolute dosimetry is nearly impossible when protons are fully stopped in the cell monolayer. As a practical consequence, low-energy protons (below $\sim 5\,\mathrm{MeV}$ in front of the irradiation system) have to be filtered out.

- Because of the biological heterogeneity and dose dependence of radiobiological effects, numerous cell samples and several independent replications of the experiments have to be performed.

- Supplementary cell samples (controls) have to be prepared but not irradiated for the determination of the impact of ambient conditions and the whole experimental procedure on the cells and on the examined biological effect.

- A cell laboratory next to the laser facility is necessary for cell culturing, sample preparation and analysis of the biological effect after irradiation. In parallel with the laser experiment, reference irradiations are required for classification of the obtained biological results and for comparison with other laboratories.

3. Establishment of laser-driven radiobiological cell irradiations

3.1. Laser–proton acceleration and beam transport

The cell irradiation experiment was performed with the ultra-short pulse 150 TW laser system, Draco (Dresden laser acceleration source), recently installed [15] at the Forschungszentrum Dresden-Rossendorf. From the Ti:sapphire system, laser pulses with an energy of about 3 J and a pulse duration of 30 fs are transported to the target area. After pulse compression the beam is focused to a focal spot of $3\,\mu\mathrm{m}$ diameter (full-width at half-maximum (FWHM)). About 80% of the laser energy is concentrated in the focal spot leading to laser peak intensities exceeding $10^{21}\,\mathrm{W\,cm^{-2}}$ on the target. The laser performance on the target is discussed in further detail in [15].

Inside the target vacuum chamber sketched in figure 1, a 2-μm-thick Ti foil is irradiated with p-polarized light at an incident angle of $50°$. Positioning of the target front surface in the focal plane is continuously monitored between consecutive laser shots by frontside imaging of the focal spot of a co-propagating alignment laser beam, resulting in an alignment precision for the focus depth of $10\,\mu\mathrm{m}$. Precise target alignment ensures a high shot-to-shot stability but limits the number of laser pulses on the target to about five per minute as a new unirradiated position on a target foil has to be addressed after every shot. In future experiments, this procedure can be improved by further automation.

Protons are accelerated from the target rear side in the target normal direction in the well-known target normal sheath acceleration (TNSA) regime, for the given laser and target parameters, again discussed in detail in [15]. The proton radiation exhibits an exponential energy distribution with a maximum energy of up to 20 MeV. The particles are emitted under a large divergence angle of about $20°$. For the higher proton energies of interest, this angle decreases and also an offset in the average emission angle from the target normal can be observed.
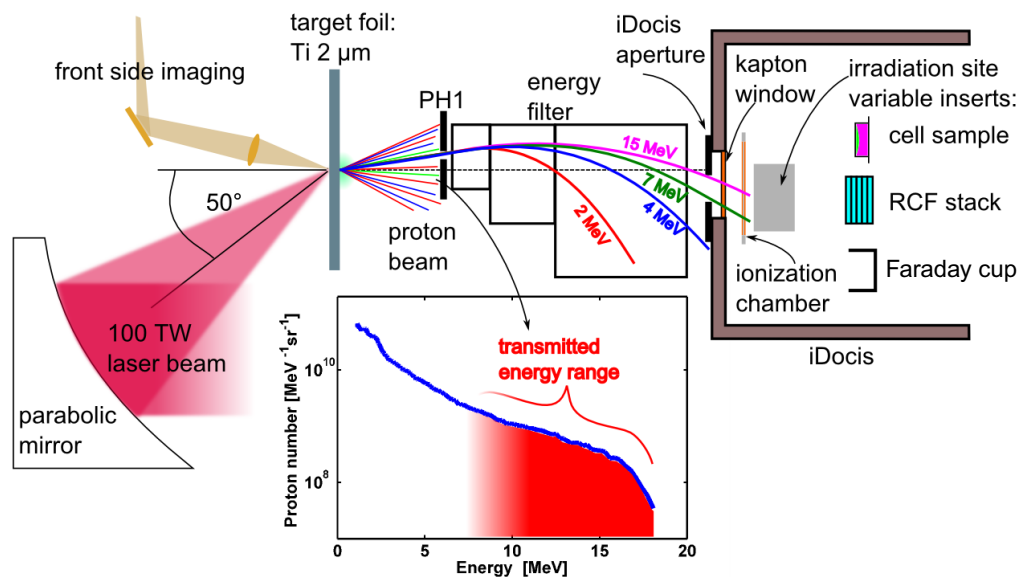
Figure 1. Schematic overview of the experimental setup, the laser proton acceleration, the proton energy filter and the integrated dosimetry and cell irradiation system (iDocis). The laser beam is focused onto a thin Ti foil and protons are accelerated from the target rear surface. In the bottom part a typical proton spectrum with a cut-off energy of 18 MeV is displayed. Protons from the energy range marked in red are transmitted through the energy filter to illuminate the irradiation site in the iDocis outside the vacuum chamber.

At a short distance of 2 cm behind the target, energetic protons enter a magnetic energy filter. The aim of this filter is the suppression of protons below energies of about 5 MeV, the efficient transport of the protons with energy of interest to the cell irradiation site and the blocking of the direct line of sight between the laser target and the irradiation site. The energy filter consists of three dipole magnet segments with increasing gap size to account for the beam divergence and an entrance pinhole (PH1, 2 mm diameter). The configuration and the positioning of the filter system have been optimized for the measured angular emission distribution, which is presented in figure 3 of [15].

Directly following the magnetic filter and thus about 20 cm downstream of the target foil, the integrated dosimetry and cell irradiation system (iDocis) is located, providing a thin kapton window at its front for the separation of its interior components for dosimetry and cell irradiation from the vacuum of the target chamber. An additional optional aperture limits the entrance area to the iDocis and is matched to the size of the samples at the downstream irradiation site (iDocis aperture, 18×5 mm^2). The entrance pinhole and aperture are shifted from the target normal axis by 1.5 mm and -7 mm, respectively, to eliminate the risk of direct x-ray irradiation of the cell samples.

For the determination of the spectral filtering properties of the full system and thus for the prediction of the proton spectrum at the location of the cell irradiation site, the representative energy spectrum of laser-accelerated protons given in the inset of figure 1 was chosen as the input for a numerical analysis. First, the magnetic field map was calculated using RADIA [19] and CST EM-Studio (Computer Simulation Technology, Darmstadt, Germany),
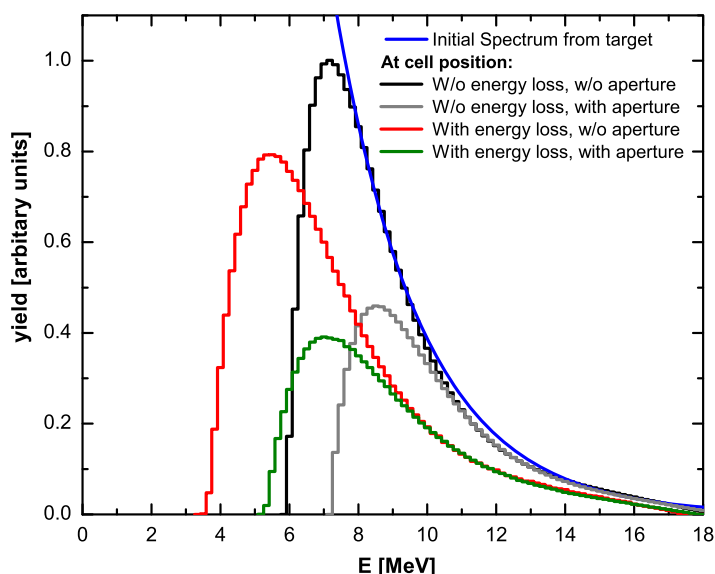
Figure 2. Simulated energy spectra at the location of the cell samples based on the measured initial spectrum presented in figure 1 (blue line) for two aperture configurations and partially including energy loss in transmitted components (red and green curves). The input spectrum is normalized to the filtered one (black curve).

resulting in good agreement. Proton trajectories were simulated by means of GPT (Pulsar Physics, Eindhoven, NL). Two different setups were treated, one without the optional iDocis aperture (black curve in figure 2) already showing an effective suppression of the proton beam components below 6 MeV, and the second including the aperture resulting in an increased low-energy cut-off (grey curve).

For the simulation of the additional energy loss of protons in the transmitted iDocis components including the vacuum window, air, the ionization chamber (IC) and the bottom of the cell vessel, these spectra were fed into a Monte-Carlo simulation using FLUKA 2008.3b-1 [19, 20]. The final energy spectra with and without the iDocis aperture at the position of the cell monolayer are presented in figure 2 as green and red lines, illustrating the significant influence of energy loss on the spectrum.

3.2. Dosimetry

The challenges regarding the dosimetry of laser-accelerated polyenergetic proton beams listed in section 2 require the development of an online dosimetry and cell irradiation device integrating different detectors that in combination and after calibration provide absolute dose information. This dedicated iDocis module integrates an IC made of ultra-thin foils for online dosimetry and a Faraday cup (FC) inset for absolute dosimetry that can be replaced by a cell holder inset for cell irradiation studies. Radiochromic films, i.e. Gafchromic EBT or CR-39 solid state nuclear track detectors, can be placed in the cell holder inset for the measurement of the 2D dose and spectral energy distribution in the plane of the cell mono layer. EBT films are also evaluated for absolute dosimetry.

The IC chamber optimized for the lowest ion energies consists of three metallized kapton foils (each only 7.5 μm thick) with a gap size of 6.6 mm and an effective diameter of 5.5 cm. It was operated at 300 V and showed a linear response against the FC [21]. As the IC is permanently placed in front of the different insets, it provides online information for all irradiation experiments (e.g. FC, EBT film or cell irradiations), allowing for a real-time control of dose delivery. The required absolute dose calibration of the IC can be performed in two independent ways: (i) it can be cross-calibrated against EBT films, or (ii) against the FC. For that purpose for both the FC and EBT/EBT-2 films, an absolute calibration was carried out before performing irradiation experiments with laser-accelerated protons [21] for proton energies of 5–60 MeV at the eye tumour therapy centre at Helmholtz Zentrum Berlin (HZB), Germany.

The design of the FC as a reference instrument was adopted from Cambria *et al* [20], with modifications at the guard ring design to improve the shielding from secondary electrons. With the readout electronics optimized for the integration of small charges independently of the time structure of the charged particle pulse, it was tested and used at several accelerators [21]. The FC calibration factor k_{FC}, defined as the ratio between deposited charge and FC amplifier signal, was determined in three independent ways: (i) electronic calibration by applying a defined charge to the FC amplifier, (ii) dose calibration against a clinically established absolute dosimetry at a clinical proton facility and (iii) a calibration with CR-39 solid state track detectors leading to a consistent calibration. With the calibration factor, the deposited dose in water can be derived from the measured FC signal M_{FC} by

$$D_{FC} = \frac{1}{A_{eff}} \frac{M_{FC} \cdot k_{FC}}{e} \frac{\int \frac{S(E)}{\rho} N(E) \mathrm{d}E}{\int N(E) \mathrm{d}E}. \tag{1}$$

Hence, the energy spectrum of the proton beam $N(E)$, the effective area of the FC A_{eff} defined in [20], the stopping power in water $S(E)/\rho$ and the calibration factor of the FC k_{FC} have to be known. The effective area is measured with EBT radiochromic films directly in front of the FC.

For the first cell irradiation series, the IC was cross-calibrated on the basis of EBT film stack irradiations. Two stacks of EBT films were irradiated before and after the cell irradiation. The cross-calibration factor of the IC was calculated from the measured dose at the cell location (5×5 mm^2) on the first film of the stack and the integrated IC signal during the irradiation of the stack. The mean cross calibration factor from both stack irradiations was finally taken to determine the absolute dose delivered to the cells from the IC signal during cell irradiation. No aperture in front of the iDocis was used to maximize the proton fluence at the cell location and to acquire maximum information on dose and energy distribution at the plane of the cell layer. As a consequence, more protons entered the iDocis and crossed the IC than were required for the irradiation of the area of the cell probe and the FC, and thus complicated the use of FCs as an independent absolute cross-calibration reference.

Combined with the iDocis aperture, another series of cell irradiation runs was performed that demonstrated the capabilities of the FC as the second dose calibration system independent of the EBT film calibration. The full analysis of this test, with special emphasis on the precise and detailed performance of the complete dosimetry system required for future radiobiological experiments, will be published elsewhere.
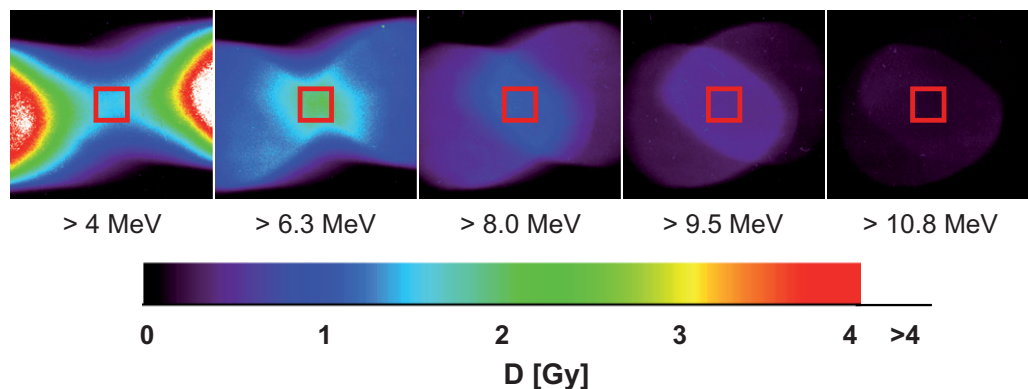
Figure 3. Dose information for an EBT film stack irradiated without iDocis aperture. The red squares mark the location of the cell sample, showing a clear maximum dose level at the second film. Without aperture, the dipole character of the energy filter, as well as the homogenizing effect of turning the stack after 5 of the 10 laser pulses, is clearly visible.

3.3. Spectral and spatial proton distribution at the cell location

An important condition for the precise control of the dose deposited into a thin monolayer of cells is that the minimum energy of the applied proton pulses does not fall below about 3 MeV to avoid the stopping of protons within the monolayer. Furthermore, the energy spectrum at the position of the monolayer has to be known for the conversion from proton fluence to dose (see equation (1)). Due to practical limitations, this spectrum cannot be measured directly when the iDocis is mounted. Therefore, we rely on the simulation of the spectrum based on a measured spectrum without iDocis, already presented in figure 2. Although the spectrum with mounted iDocis aperture provides a better energy selection (minimum energy 5.3 MeV), the spectrum without aperture also fulfils the requirements for cell irradiation in terms of minimum energy (3.5 MeV), and has the advantage of a higher total proton number. Thus, this configuration was chosen for the first irradiation of cell probes.

EBT radiochromic film stacks were used to determine both spectral and spatial proton dose distributions at the location of the cell probes. In figure 3, the dose information from one representative film stack is given. Note that for a further homogenization of the spatial dose distribution, for a single pulse reflecting the correlation between proton energy and deflection angle in the dipole filter, the film stacks as well as the cell probes are rotated by 180° after half of the applied laser pulses. Nevertheless, the spatial energy separation expected from the magnetic filtering can be seen, especially on the first films. The dose at the location of the cell sample, marked by the red square, increases from the first to the second film, which is due to a Bragg peak of protons with energies greater than 6 MeV. Thus, dominantly high-energy protons with energies larger than 6 MeV reach the irradiation site, being well in agreement with the expected spectrum shown as a red line in figure 2. Furthermore, the dose homogeneity at the cell location can be determined from the first EBT film of the stack. It was found to be ±9% for a 95% confidence level for the two irradiated stacks.

3.4. Cell irradiation

The experiments were performed with the radiosensitive squamous cell carcinoma (SCC) cell line SKX. SKX was initially established as a xenograft line in nude mice from a biopsy of a moderately squamous cell carcinoma of the floor of the mouth. The *in vitro* cell line SKX was established from the xenograft line and is described in detail in [22]–[25]. SKX as cultivated in Dulbecco's minimum essential medium with $4.5\,g\,l^{-1}$ stable glutamin (Biochrom AG, Berlin, Germany) containing 10% FBS (Sigma-Aldrich Chemie GmbH, Taufkirchen, Germany), 1 mM sodium pyruvate, 20 mM HEPES, 1% $100\times$ non-essential amino acids (all from PAA) and 1% Penicillin/streptomycin (Biochrom). Cells were seeded one day before irradiation at a density of $175\times10^2\,cells\,cm^{-2}$ on a thin biofilm (lumox®, 50 μm thickness) at the bottom of a 4-well slide (Sarstedt AG and Co., Nümbrecht, Germany). The lumox 4-well slide was chosen as a result of the optimization of cell culture conditions, staining procedure, minimal energy loss in the vessel bottom and a compromise between beam spot size and cell target size. By seeding cells in one well of the slide, an area of $5\times5\,mm^2$ is covered by the cell monolayer and positioned in the horizontal proton beam (cf figure 3). Before irradiation, 1 ml of cell culture medium was added and the well was closed with sterile Parafilm® to ensure vertical orientation of the 4-well slides during irradiation. Immediately after irradiation the cell culture medium was completely changed and the cells were incubated for an additional 24 h (37 °C, 5% CO_2, 95% humidification) to allow for the repair of sublethal damage. For the detection of residual DNA double-strand breaks, the immunofluorescence γ-H2AX/53BP1 staining technique was used, which is well established in our laboratory and described in [23, 26].

In the presented experiment, three cell samples were irradiated with different doses, delivering low, medium and high doses by applying 12, 20 and 29 laser-accelerated proton pulses, respectively. After half of the prescribed dose level was reached, the cell sample was rotated by 180° to homogenize the dose distribution at the cell position, as discussed in figure 3.

In figure 4, the shot-to-shot dose reproducibility measured with the IC as an online dose monitor is shown. With a stable mean dose per shot of (0.137 ± 0.039) Gy during cell and EBT stack irradiation, the proton beam exhibits a long-term stable dose-per-pulse characteristic with shot-to-shot variations of about $\pm28\%$ for a 95% confidence level. This measurement demonstrates a remarkably reliable operation of the laser-driven proton source and thus confirms stable laser conditions on the target.

As the IC provides the online dose information for every applied pulse, the delivery of the prescribed doses to the cell samples is possible with a maximum uncertainty in units of the dose of one pulse. Moreover, the influence of saturation of the IC can be neglected, as the IC is calibrated against a dose-rate-independent dosimeter at a similar signal amplitude and the pulse-to-pulse fluctuations are moderate.

In figure 5, the results of the double-strand break staining are shown for one representative cell nucleus of each of the cell samples irradiated with 1.5, 2.7 and 4.1 Gy, respectively. An increase in the number of DNA double-strand breaks is observed with an increased dose, indicating the dose-effect of the biological damage to the tumour cells. The uncertainty in dose can be estimated to be about 20% (9% homogeneity, 4% film calibration and 7% energy dependence).
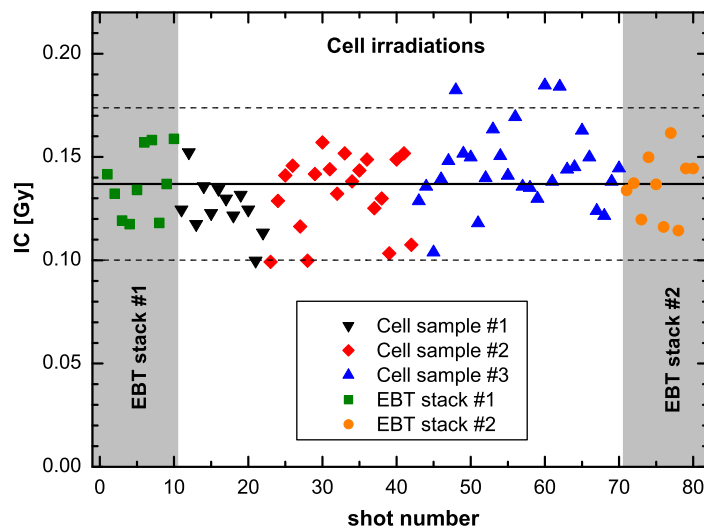
Figure 4. Shot-to-shot dose variations over all EBT film stack and cell irradiations. The mean dose rate of 0.137 Gy for all irradiation is shown as a black solid line, whereas the 2σ confidence band is indicated with dashed lines.
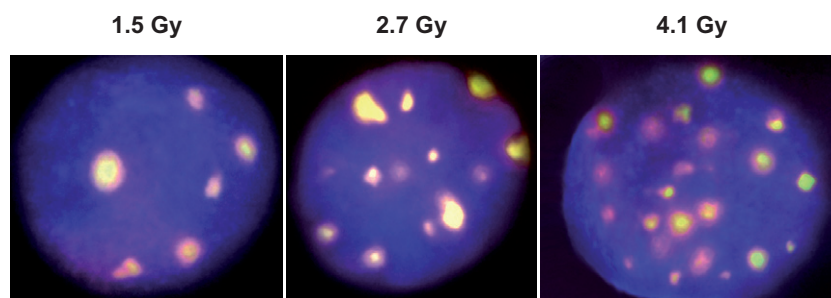

Figure 5. Fluorescence microscopy view (1000-fold magnification) of SKX tumour cell nuclei irradiated with different doses delivered by laser-accelerated protons. Each formation of co-localized γ-H2AX plus 53BP1 foci (coloured yellow-pink) indicates a double-strand break, whereas DAPI staining of the DNA (coloured blue) allows its localization in the cell nucleus, which is about $10\,\mu$m in diameter.

4. Conclusion

The presented controlled *in vitro* cell irradiation by laser-accelerated protons represents an important milestone on the path to the development of laser ion acceleration for clinical radiotherapy. All the key requirements for radiobiological cell experiments have been fulfilled, such as the construction of a versatile cell irradiation module, the supply of a stable particle beam providing precise dose delivery in an appropriate irradiation time and on a macroscopic irradiation field, online dose monitoring for irradiation control and the precise determination of the absolute proton dose.

As the next step, comprehensive radiobiological experiments, such as the determination of complete dose–effect curves for several tumour and normal tissue cell lines will be performed, yielding the biological effectiveness of laser-accelerated proton beams.

    In parallel, the laser-accelerated proton beam will be improved with respect to maximum energy, as well as to spectral and spatial distribution in order to enable radiobiological animal experiments in a subsequent step. The required maximum proton energy for this step of a few 10 MeV will probably be reachable with the 100 TW class laser Draco and envisioned upgrades.

    For future therapeutic applications, a further increase in the proton energy of up to 250 MeV is necessary. Based on established experimental results (see, e.g., [12, 15]), no straightforward solution to this quest can be given. Ongoing development of laser technology, especially in the field of compact PW class systems, in the use of micro-structured targets and in the investigation of alternative laser plasma-based acceleration regimes, not only offers promising approaches for reaching this goal, but may also lead to an improved quality of the proton spectra [27]–[29].

Acknowledgments

References

[1] Debus J, Haberer T, Schulze-Ertner D, Jäkel O, Wenz F, Enghardt W, Schlegel W, Kraft G and Wannenmacher M 2000 Fractionated carbon ion irradiation of skull base tumors at GSI. First clinical results and future perspectives *Strahlenther. Onkol.* **176** 211–6

[2] Durante M and Loeffler J S 2010 Charged particles in radiation oncology *Nat. Rev. Clin. Oncol.* **7** 37–43

[3] Schardt D, Elsässer T and Schulz-Ertner D 2010 Heavy-ion tumor therapy: physical and radiobiological benefits *Rev. Mod. Phys.* **82** 383–425

[4] Durante M 2008 Focus on heavy ions in biophysics and medical physics *New J. Phys.* **10** 075002

[5] Snavely R A *et al* 2000 Intense high-energy proton beams from petawatt-laser irradiation of solids *Phys. Rev. Lett.* **85** 2945–8

[6] Bulanov S V and Khoroshkov V S 2002 Feasibility of using laser ion accelerators in proton therapy *Plasma Phys. Rep.* **28** 453–6

[7] Bulanov S V, Esirkepov T Z, Khoroshkov V S, Kunetsov A V and Pegoraro F 2002 Oncological hadrontherapy with laser ion accelerators *Phys. Lett.* A **299** 240–247

[8] Fourkal E, Li J S, Ding M, Tajima T and Ma C-M 2003 Particle selection for laser-accelerated proton therapy feasibility study *Med. Phys.* **30** 1660–70

[9] Ledingham K W D, McKenna P and Singhal R P 2003 Applications for nuclear phenomena generated by ultra-intense lasers *Science* **300** 1107–111

[10] Malka V *et al* 2004 Practicability of protontherapy using compact laser systems *Med. Phys.* **31** 1587–92

[11] Ma C M, Veltchev I, Fourkal E, Li J. S, Luo W, Fan J, Lin T and Pollack A 2006 Development of a laser-driven proton accelerator for cancer therapy *Laser Phys.* **16** 639–46

[12] Ledingham K W D and Galster W 2010 Laser-driven particle and photon beams and some applications *New J. Phys.* **12** 045005

[13] Ledingham K W D, Galster W and Sauerbrey R 2007 Laser-driven proton oncology—a unique new cancer therapy? *Br. J. Radiol.* **80** 855–858

[14] Linz U and Alonso J 2007 What will it take for laser driven proton accelerators to be applied to tumor therapy? *Phys. Rev. Special Topics—Accelerators Beams* **10** 094801

[15] Zeil K, Kraft S D, Bock S, Bussmann M, Cowan T E, Kluge T, Metzkes J, Richter T, Sauerbrey R and Schramm U 2010 Scaling of proton energies in ultra-short pulse laser plasma acceleration *New J. Phys.* **12** 045015

[16] Beyreuther E *et al* 2010 Establishment of technical prerequisites for cell irradiation experiments with laser-accelerated electrons *Med. Phys.* **37** 1392–1400

[17] Yogo A *et al* 2009 Application of laser-accelerated protons to the demonstration of DNA double-strand breaks in human cancer cells *Appl. Phys. Lett.* **94** 181502

[18] Schmid T E, Dollinger G, Hable V, Greubel C, Zlobinskaya O, Michalski D, Molls M and Röper B 2010 Relative biological effectiveness of pulsed and continuous 20 MeV protons for micronucleus induction in 3D human reconstructed skin tissue *Radiother. Oncol.* **95** 66

[19] Elleaume P, Chubar O and Chavanne J 1997 Computing 3D magnetic field from insertion devices *Proc. PAC97 Conf.* pp 3509–11

[20] Cambria R, Hérault J, Brassart N, Silari M and Chauvel P 1997 Proton beam dosimetry: a comparison between the faraday cup and an ionization chamber *Phys. Med. Biol.* **42** 1185

[21] Richter C *et al* unpublished

[22] Dörfler A, Eicheler W, Zips D, Petersen C and Baumann M 2000 Establishment and characterization of the radiosensitive squamous cell carcinoma line SKX *in vitro* (in German) *Exp. Strahlenther. Klin. Strahlenbiol.* **9** 11–13

[23] Menegakis A, Yaromina A, Eicheler W, Dörfler A, Beuthien-Baumann B, Thames H D, Baumann M and Krause M 2009 Prediction of clonogenic cell survival curves based on the number of residual DNA double strand breaks measured by γH2AX staining *Int. J. Radiat. Biol.* **85** 1032–41

[24] Kasten-Pisula U *et al* 2009 The extreme radiosensitivity of the squamous cell carcinoma SKX is due to a defect in double-strand break repair *Radiotherapy Oncol.* **90** 257–64

[25] Eicheler W, Zips D, Dörfler A, Grénman R and Baumann M 2002 Splicing mutations in TP53 in human squamous cell carcinoma lines influence immunohistochemical detection *J. Histochem. Cytochem.* **50** 197–204

[26] Beyreuther E, Lessmann E, Pawelke J and Pieck S 2009 DNA double strand breaks signaling: X-ray energy dependence residual co-localised foci of γ-H2AX and 53BP1 *Int. J. Radiat. Biol.* **85** 1042–50

[27] Schwoerer H, Pfotenhauer S, Jäckel O, Amthor K-U, Liesfeld B, Ziegler W, Sauerbrey R, Ledingham K W D and Esirkepov T 2006 Laser–plasma acceleration of quasi-monoenergetic protons from microstructured targets *Nature* **439** 445

[28] Hegelich B M, Albright B J, Cobble J, Flippo K, Letzring S, Paffett M, Ruhl H, Schreiber J, Schulze R K and Fernandez J C 2006 Laser acceleration of quasi-monoenergetic MeV ion beams *Nature* **439** 441–4

[29] Gaillard S A *et al* Laser-accelerated protons above 65 MeV, resulting from a novel laser–cone interaction mechanism unpublished